Experimental evidence of modal wavenumber relation to zeros in the wavenumber spectrum of a simply supported plate

Olivier Robin, Alain Berry, Noureddine Atalla, et al.

Citation: The Journal of the Acoustical Society of America **137**, 2978 (2015); doi: 10.1121/1.4919334
View online: https://doi.org/10.1121/1.4919334
View Table of Contents: https://asa.scitation.org/toc/jas/137/5
Published by the Acoustical Society of America

Experimental evidence of modal wavenumber relation to zeros in the wavenumber spectrum of a simply supported plate (L)

Olivier Robin,[a] Alain Berry, and Noureddine Atalla
Groupe d'Acoustique de l'Université de Sherbrooke, Université de Sherbrooke, Sherbrooke J1K 2R1, Canada

Stephen A. Hambric and Micah R. Shepherd
Applied Research Laboratory, The Pennsylvania State University, P.O. Box 30, State College, Pennsylvania 16804, USA

(Received 25 February 2015; revised 6 April 2015; accepted 11 April 2015)

The modal wavenumber of rectangular, simply supported, isotropic thin plates was theoretically shown to be related to the zeros in the wavenumber spectrum and not to the peaks, resulting in an error between the actual modal wavenumber and location of the wavenumber spectrum peak for low mode orders. This theoretical proof is confirmed by experimental results reported in this letter.
 [http://dx.doi.org/10.1121/1.4919334]

[NJK] Pages: 2978–2981

I. INTRODUCTION

The squared magnitude of the spatial Fourier transform of the mode shape function of a structure is usually called the wavenumber sensitivity function or wavenumber filter shape function, and is often used to calculate the coupling between exciting pressure fields and mode shapes for rectangular panels[1–4] and cylinders,[5,6] both under fluctuating wall pressure excitations. It can be also used to calculate the radiation efficiency of rectangular panels in the wavenumber domain.[3] It is often stated that this function precisely peaks at the modal wavenumber and that the highest sensitivity or coupling with an exciting pressure field will thus be found at this wavenumber.[1–3,7]

Shepherd and Hambric[8] have theoretically shown that the modal wavenumber is related to the zeros and not to the peaks in the wavenumber spectrum in the case of a rectangular, simply supported, isotropic thin panel. To the best of the authors' knowledge, no exhaustive laboratory validation of this analytical proof or confirmation of the calculated percentage differences between modal wavenumber and peak wavenumber can be found in the literature. This result was only briefly confirmed for a single vibration mode of such a panel in Ref. 9. Using a measurement database obtained with a similar laboratory setup,[10] the main contribution of this letter is to provide a comprehensive experimental validation of Shepherd and Hambric's result.

II. DESCRIPTION OF TESTS AND WAVENUMBER SPECTRUM CALCULATIONS

For a thin, simply supported and isotropic panel, the mode shape (or eigenfunction) Ψ_{mn} and eigenfrequency ω_{mn}, solutions of the free vibration equation take simple closed-form expressions:

$$\Psi_{mn}(x,y) = \sin(k_m x)\sin(k_n y), \tag{1}$$

where the modal wavenumbers are

$$k_m = \frac{m\pi}{L_x}, \quad k_n = \frac{n\pi}{L_y}, \tag{2}$$

and

$$\omega_{mn} = \left(\frac{D}{\rho h}\right)^{1/2}\left[\left(\frac{m\pi}{L_x}\right)^2 + \left(\frac{n\pi}{L_y}\right)^2\right], \tag{3}$$

where D is the bending stiffness, ρ is the mass density, h the panel thickness, m and n are non-zero strictly positive integers, and L_x and L_y are the panel length and width, respectively. The discrete form of the 2D spatial Fourier transform $S_{mn}(k_x, k_y)$ of the mode shape function is

$$S_{mn}(k_x,k_y) = \Delta_x\Delta_y \sum_{k=1}^{N_x}\sum_{l=1}^{N_y} \Psi_{mn}(x_k,y_l)e^{-jk_x x_k}e^{-jk_y y_l}, \tag{4}$$

where Δ_x and Δ_y are the spatial samplings in the x and y directions, respectively. For $m, n = 1$, the main lobe of $S_{mn}(k_x, k_y)$ [or of the sensitivity function $|S_{mn}(k_x, k_y)|^2$] peaks at $(k_x, k_y) = 0$.[1,7] For $m, n > 1$, it is often stated that the two main lobes in the k_x and k_y directions peak at the modal wavenumbers $k_m = \pm(m\pi/L_x)$ and $k_n = \pm(n\pi/L_y)$, respectively.

Figure 1 shows the experimental setup. A simply supported rectangular panel of dimensions 0.48 m × 0.42 m, thickness $h = 3.19$ mm, made of aluminum (bending stiffness $D = 270.5$ N m, mass density $\rho = 2720$ kg/m^3), was placed over a weighted base, baffled and installed in an anechoic chamber. Representative experimental simply supported boundary conditions, already validated in previous works,[9,10] were achieved by gluing the plate edges to thin vertical supports in order to obtain a small rotational stiffness and a high transversal stiffness (ideal simply supported boundary conditions imply a null rotational stiffness and an infinite transversal stiffness, so that any edge can rotate freely while being restricted from out-of-plane displacements). A volume velocity acoustic source (LMS mid-high frequency volume source) was positioned at $x = 0.36$ m and $y = 0.12$ m, in front of the baffled panel at a distance $z = 5.1$ cm in the coordinate system shown in Fig. 1. Its termination includes a sensor which provides a

[a]Electronic mail: olivier.robin@usherbrooke.ca

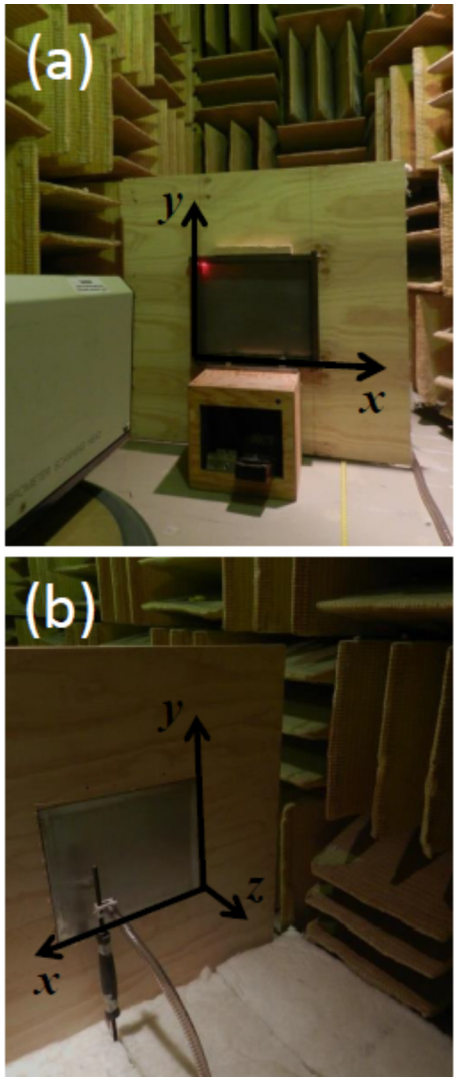

FIG. 1. (Color online) Experimental set-up showing the baffled panel in an anechoic chamber and co-ordinate axes. (a) Laser Doppler velocimetry measurement, (b) volume source excitation.

direct measurement of its volume velocity. The transverse velocity of the panel was measured on a regular grid of 37×27 points over the panel surface (excluding panel edges), using a Polytec scanning laser vibrometer for a white noise input of the acoustic source in the 170–2000 Hz range with a frequency resolution of 0.625 Hz (the lower frequency limit is intrinsic to low frequency limitations of the acoustic source).

An average structural loss factor $\eta = 0.004$ was experimentally determined using the -3 dB bandwidth method on the few first resonances of the plate. For such a small loss factor, it is assumed that the resonant response of the panel under acoustical excitation will only include the corresponding vibration mode. The operational mode shapes identified at each resonance frequency were also considered identical to plate mode shapes, and the data used for calculations were finally the plate displacement response to a unitary volume velocity of the source at each experimental resonance frequency. The operational mode shapes were then normalized to have a maximum equal to unity [as for theoretical mode shapes, see Eq. (1)].

To obtain these operational mode shapes and calculate corresponding 2D spatial Fourier transforms, the measured velocity response was first converted to displacement through division by $j\omega$ for each studied frequency. Additional zero displacement points were then imposed along panel edges finally leading to a regular $N_x = 39 \times N_y = 29$ grid, with corresponding spatial samplings of $\Delta_x = 1.26$ cm in the x direction, and $\Delta_y = 1.5$ cm in the y direction. The measured displacement response was zero-padded in both x and y directions in order to increase wavenumber resolution. The total number of points W_xN_x and W_yN_y in x and y directions were chosen so as to provide imposed wavenumber resolutions $\Delta_{kx} = 2\pi/W_xN_x\Delta_x$ and $\Delta_{ky} = 2\pi/W_yN_y\Delta_y$. The results presented were obtained using padding factors of $W_x = 100$ in the x direction and $W_y = 114$ in the y direction (the aspect ratio of the panel is 1.14), so that a wavenumber resolution of 0.131 rad/m was obtained in both directions. The highest wavenumbers that are resolved without aliasing effects are $k_{x_{\max}} = \pm\pi/\Delta_x = \pm 249.3$ rad/m and $k_{y_{\max}} = \pm\pi/\Delta_y = \pm 209.4$ rad/m. The discrete wavenumbers are thus defined in the range $[-k_{x_{\max}}; +k_{x_{\max}}] \times [-k_{y_{\max}}; +k_{y_{\max}}]$ with a uniform 0.131 rad/m wavenumber resolution.

III. EXPERIMENTAL RESULTS

Figure 2 shows the theoretical eigenfrequencies [see Eq. (3)] versus the measured resonance frequencies for mode orders up to $m = 7$ and $n = 6$ along the panel's length and width, respectively. The agreement between theoretical eigenfrequencies and measured resonance frequencies is very satisfactory, with the highest percentage difference of 3.4% obtained for mode (2,1) and lower or equal to 2% for all the other modes (similar results were reported in Refs. 9 and 10). Excluding the modes that were not located within the measurement bandwidth [such as the fundamental (1, 1) mode at a frequency of 77 Hz], and those that were not properly identified, a set of 29 modes was finally used to calculate experimental 2D wavenumber transforms using Eq. (4).

Figures 3(a)–3(c) show experimental and theoretical results in the wavenumber domain for the resonance frequency corresponding to the (5, 2) mode. Figure 3(a) shows the calculated sensitivity function $|S_{mn}(k_x, k_y)|^2$ from measurements for this mode in the (k_x, k_y) plane. Figures 3(b) and 3(c) show results for the same mode obtained from operational and

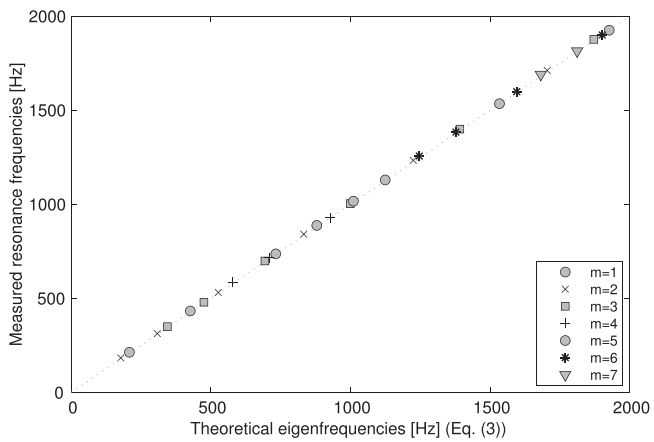

FIG. 2. Theoretical eigenfrequencies versus measured resonance frequencies of the tested aluminum panel with the corresponding modal index m (only this index is indicated for clarity).

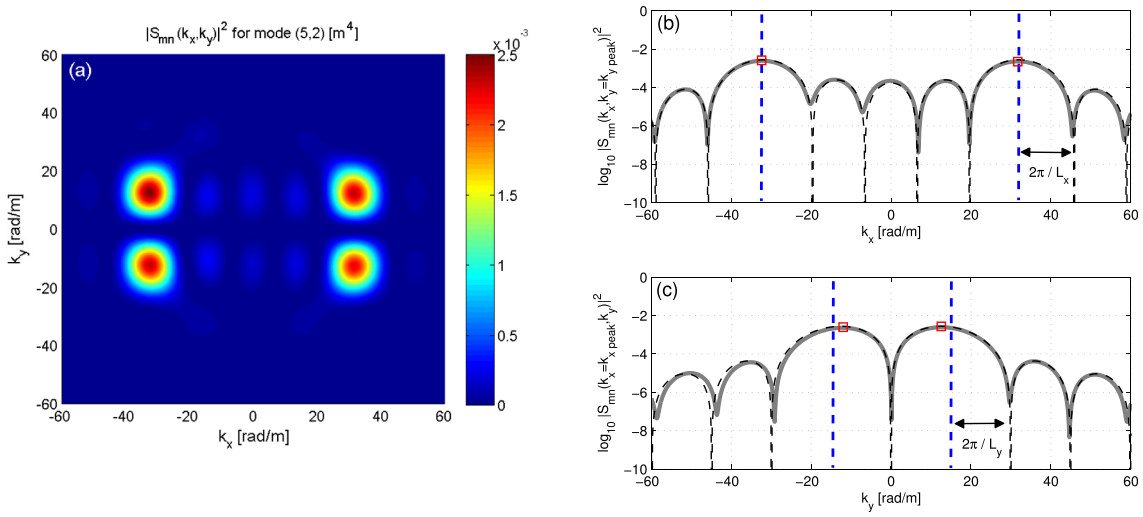

FIG. 3. (Color online) Experimental and theoretical results for the (5, 2) mode: (a) measured sensitivity function $|S_{mn}(k_x, k_y)|^2$ in the (k_x, k_y) plane; (b) plot in the k_x direction of $\log_{10}|S_{mn}(k_x, k_y = k_{y\,peak})|^2$ for operational (thick continuous gray line) and theoretical mode shapes (thin dashed black line); (c) plot in the k_y direction of $\log_{10}|S_{mn}(k_x = k_{x\,peak}, k_y)|^2$ for operational (thick continuous gray line) and theoretical mode shapes (thin dashed black line). Boxes indicate peak wavenumbers, while vertical dashed lines indicate theoretical modal wavenumbers.

theoretical mode shapes [Eq. (1)], but plotted as cuts in the k_x and k_y directions, respectively. The sensitivity functions obtained with operational and theoretical mode shapes are in good agreement. In Figs. 3(b) and 3(c), the theoretical modal wavenumbers and experimental peak wavenumbers are also indicated by vertical dashed lines and boxes, respectively. The deviation between modal wavenumber and peak wavenumber for both experimental and theoretical calculations is clearly visible on Fig. 3(c). Since the sensitivity function approaches zero rapidly, the wavenumber transform does not exactly

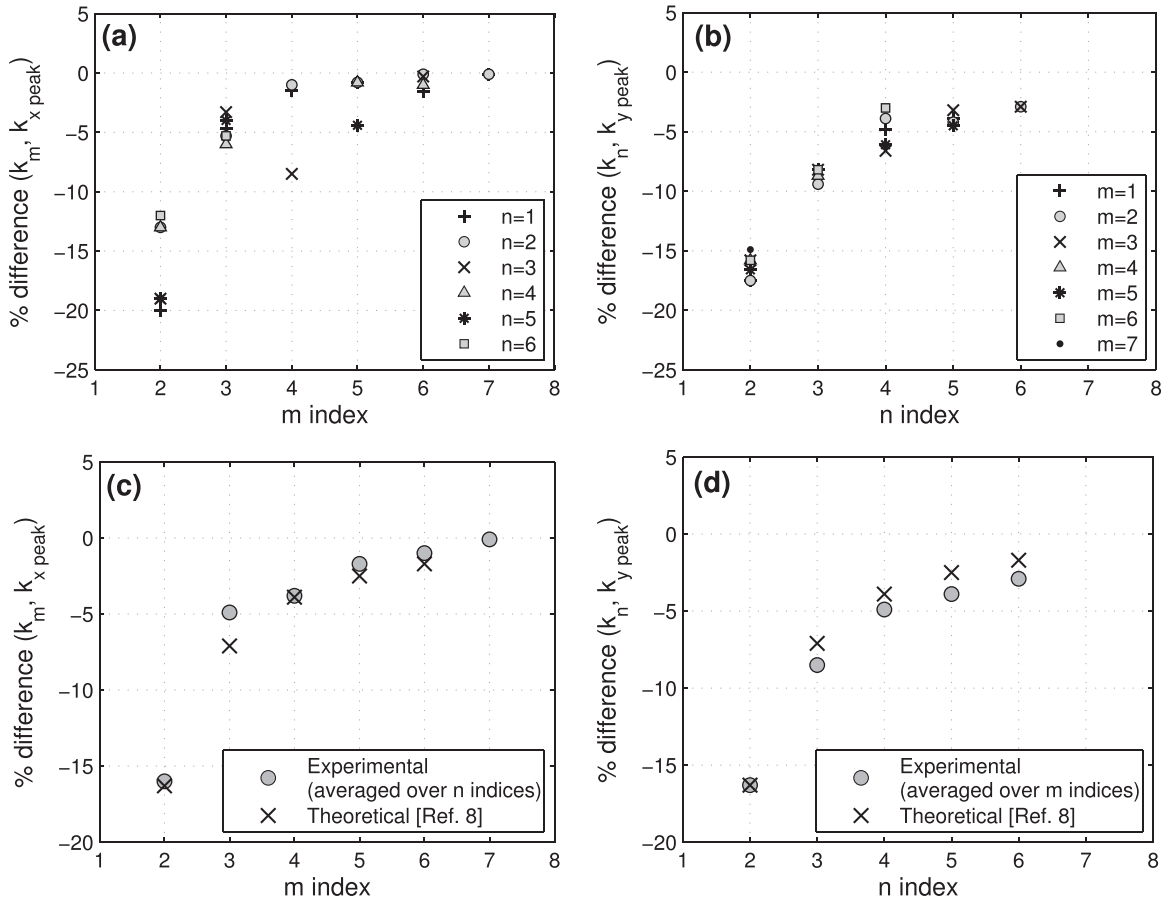

FIG. 4. (a) Percentage difference between modal and peak wavenumbers versus modal index m for various n indices. (b) Percentage difference between modal and peak wavenumbers versus modal index n for various m indices. (c) Mean experimental percentage difference for each index m mode compared to theoretical results of Ref. 8. (d) Mean experimental percentage difference for each index n compared to theoretical results of Ref. 8.

capture the location of the zero due to it is finite resolution. If insufficient zero padding is performed, the zero may not be resolved and the modal wavenumber estimate will be biased.

The (k_x, k_y) coordinates of the peak of the sensitivity function were then extracted in the $[0 < k_x; 0 < k_y]$ domain and compared to the theoretical modal wavenumbers in terms of an algebraic percentage difference, $100\ (k_{xy\ peak} - k_{mn})/k_{mn}$ (so that a negative value indicates that the measured peak wavenumber is smaller than the theoretical modal wavenumber).

With the previously defined wavenumber resolution (0.131 rad/m), the smallest percentage difference that can be estimated equals $\pm 13.1/k_{mn}\%$. Note that for the $m,\ n = 1$ case, the measured wavenumber values are very small and rounded to zero so that the percentage difference is always 100% (not shown).

Figures 4(a)–4(d) summarize the results obtained. Figure 4(a) presents the measured percentage differences versus modal index m for various modal indices n, while Fig. 4(b) presents results versus modal index n for various modal indices m. Despite some divergence [as for the mode (4, 3) in Fig. 4(a) with a large deviation of 8.5%], all the individual percentage differences for each modal index m or n are in the same range. Figures 4(c) and 4(d) then compare the mean percentage differences for each modal index m or n to the theoretical results obtained by Shepherd and Hambric.[8] The agreement between experimental mean percentage differences and theoretical predictions is very satisfactory. It is also confirmed that the percent difference between the peak wavenumber and the modal wavenumber decreases when the mode order increases, with a difference lower that 3% for (m, n) modes orders higher than 5 (note that slightly larger errors were generally found for n indices, but no explanation was found).

As suggested in Shepherd and Hambric,[8] the actual modal wavenumber for lower-order modes should be determined by adding $2\pi/L_x$ (or $2\pi/L_y$ depending on the considered dimension) to the wavenumber at the first zero preceding the maximum wavenumber or subtracting the same quantity from the wavenumber at the first zero after the peak [as illustrated in Figs. 3(b) and 3(c)]. This especially stands for unitary mode orders ($m,\ n = 1$), for which the wavenumber spectrum peaks at $(k_x, k_y) = 0$. For mode (1, 3), as an example, the first zero following the peak centered on zero along the k_x axis (for $m = 1$) is found at 19.9 rad/m. Applying the suggested computation leads to a value of 6.81 rad/m for the actual modal wavenumber, with a percentage difference between theoretical modal wavenumber and experimentally determined modal wavenumber of 4.1%.

IV. CONCLUSION

Following a previous theoretical analysis[8] of the wavenumber spectrum of simply supported, isotropic rectangular thin plate flexural modes that revealed an error concerning the location of the modal wavenumber, an experimental validation of this result was conducted. Using 2D laser Doppler velocimetry measurements on a simply supported rectangular panel excited by a distributed acoustic excitation, 29 flexural modes were identified and corresponding mode shapes were spatial Fourier transformed. The results obtained confirm that (1) the modal wavenumber is related to the zeros in the wavenumber spectrum, (2) the percent difference between the peak wavenumber and the modal wavenumber is non-negligible at low wavenumbers ($m,\ n \leq 5$) but becomes small for higher wavenumbers, and (3) the measured differences are in good agreement with those of Shepherd and Hambric.

[1]N. C. Martin and P. Leehey, "Low wavenumber wall pressure measurements using a rectangular membrane as a spatial filter," J. Sound Vib. **52**(1), 95–120 (1977).

[2]Y. F. Hwang and G. Maidanik, "A wavenumber analysis of the coupling of a structural mode and flow turbulence," J. Sound Vib. **142**(1), 135–142 (1990).

[3]P. G. Bremner and J. F. Wilby, "Aero-vibro-acoustics: Problem statement and methods for simulation-based design solutions," in *Proceedings of the 8th AIAA/CEAS Aeroacoustics Conference*, AIAA Paper No. 2002-1551 (2002), pp. 1–11.

[4]S. A. Hambric, Y. F. Hwang, and W. K. Bonness, "Vibrations of plates with clamped and free edges excited by low-speed turbulent boundary layer flow," J. Fluid Struct. **19**, 93–110 (2004).

[5]N. D. Evans, D. E. Capone, and W. K. Bonness, "Low-wavenumber turbulent boundary layer wall-pressure measurements from vibration data over smooth and rough surfaces in pipe flow," J. Sound Vib. **332**, 3463–3473 (2013).

[6]W. K. Bonness, D. E. Capone, and S. A. Hambric, "Low-wavenumber turbulent boundary layer wall-pressure measurements from vibration data on a cylinder in pipe flow," J. Sound Vib. **329**, 4166–4180 (2010).

[7]F. Fahy and P. Gardonio, *Sound and Structural Vibration: Radiation, Transmission and Response*, 2nd ed. (Academic, Oxford, UK, 2007), pp. 181–183.

[8]M. R. Shepherd and S. A. Hambric, "Comment on plate modal wavenumber transforms in *Sound and Structural Vibration* [Academic Press (1987, 2007)] (L)," J. Acoust. Soc. Am. **132**(4), 2155–2157 (2012).

[9]O. Robin, A. Berry, and S. Moreau, "Experimental vibroacoustic testing of plane panels using synthesized random pressure fields," J. Acoust. Soc. Am. **135**(6), 3434–3445 (2014).

[10]A. Berry, O. Robin, and F. Pierron, "Identification of dynamic loading on a bending plate using the virtual fields method," J. Sound Vib. **333**(26), 7151–7164 (2014).